Supplemental Data

Local Retinal Circuits of Melanopsin-Containing Ganglion Cells Identified by Transsynaptic Viral Tracing

Tim James Viney, Kamill Balint, Daniel Hillier, Sandra Siegert, Zsolt Boldogkoi, Lynn W. Enquist, Markus Meister, Constance L. Cepko, and Botond Roska

Supplemental Experimental Procedures

PRV Labeling

GFP-expressing pseudorabies virus (PRV) 152 [S1] and RFP-expressing PRV 614 (kindly provided by B.W. Banfield) [S2] Bartha strains were harvested from the PK-15 cell line as described earlier [S1]. To create the PRV expressing the membrane-targeted green fluorescence protein (memGFP), we used the first 40 amino acids of the myristoylated alanine-rich C kinase substrate (MARCKS) protein fused with GFP [S3] under control of the cytomegalovirus (CMV) immediate-early promoter. The CMV-memGFP expression cassette was placed into the putative latency-associated transcript promoter (P_{LAT2}) [S4] of the PRV Bartha strain. All the PRV work was done in a biosafety level 2 laboratory. C57BL/6J mice that were 6–8 weeks old were injected with 10^3–10^5 plaque-forming units of PRV152 in 1 μl Dulbecco's Modified Eagle's Medium (DMEM) into the AntC of the right eye under isoflurane anesthesia (2% in oxygen). Animal experiments have been approved by the local Institutional Animal Care and Use Committee at Harvard and the Friedrich Miescher Institute. Animal experiments have been conducted according to the guidelines of the U.S. National Institutes of Health and the Swiss National Foundation. The cornea was punctured with a 27–28 gauge needle, and PRV152 was injected into the anterior chamber (AntC) with a 10 μl Hamilton syringe fitted with a 33 gauge needle. For labeling ganglion cells that projected to the superior colliculus (SC) or to the lateral geniculate, we performed stereotaxic surgery. We injected 10^4 plaque-forming units of PRV152 in 100 nanoliter DMEM into either the SC or V1. Animals were kept in the same laboratory for up to 150 hr after injection.

Immunohistochemistry

The retina was fixed in 4% paraformaldehyde in phosphate-buffered saline (PBS) at pH 7.4 for 30 min either after electrophysiological recordings or directly after eye enucleation and incubated at 4°C for 1–5 days. For vibratome sectioning, the retina was embedded in 2% agar in PBS and cut into 100–200-μm-thick sections with a Leica VT 1000 S vibratome. For cortical slides, the whole brain was embedded in 2% agar in PBS and vibratome sectioned into 200-μm-thick sections. The antibody-staining procedures for both whole-mount and vibratome sections were the same and were carried out at room temperature. The retina was blocked for 1 hr in 10% normal goat serum (NGS) or normal donkey serum (NDS), 1% bovine serum albumin (BSA), and 0.5% Triton X-100 in PBS (pH 7.4); incubation with the primary antibodies in 3% NGS (or NDS), 1% BSA, and 0.5% Triton X-100 in PBS for 3 days followed. After three rounds of 10–20 min washes in PBS, the secondary antibodies were applied for 2 hr in 2–10 μg/ml DAPI, 3% NGS (or NDS), 1% BSA, and 0.5% Triton X-100 in PBS. For GFP immunohistochemistry after secondary-antibody incubation, the retina was washed three times in PBS as before and incubated overnight with streptavidin conjugated to Alexa 488 (Invitrogen) in 0.5% Triton X-100 in PBS. At the end of the staining procedure, the retina was washed three times in PBS and mounted with ProLong antifade mounting medium (Invitrogen). The following primary antibodies were used: rabbit anti-GFP (1:200 or 1:500, Invitrogen), sheep anti-GFP (1:200, Biogenesis), rabbit anti-melanopsin (1:5000, kind gift from I. Provencio, Uniform Services University, Bethesda, MD), mouse anti-calretinin (1:2000, Chemicon), and mouse anti-glutamine synthetase (1:200, Chemicon). Secondary antibodies were conjugated with Biotin (for GFP staining), Alexa 488, or Alexa 633 (Invitrogen).

For double labeling, rabbit anti-GFP was used together with mouse primary antibodies, NGS-containing blocking solution, and goat secondary antibodies. Sheep anti-GFP was used together with rabbit primary antibodies, NDS-containing blocking solution, and donkey secondary antibodies.

Confocal Microscopy and Analysis

The 405, 488, and 633 nm laser lines of a Zeiss LSM 510 Meta confocal microscope were used to excite DAPI, Alexa 488, and Alexa 633, respectively. To determine the dendritic depths of PRV-labeled ganglion cells, we acquired confocal stacks of 170 ganglion cells with an automatic stage controlled by Auto Time Series Macro software [S5]. In each imaging session, 20–30 ganglion cells per retina were marked, and confocal stacks [S5] were acquired at each location. We used a 63× 1.4 numerical-aperture oil-immersion lens (Zeiss). The z steps were 0.2–0.35 μm. The scan started at the ganglion-cell layer and continued until the photoreceptor layer. The depth of dendritic ramification for each labeled ganglion cell was determined from the DAPI and Alexa 488 stacks. In brief, the dendritic depths were automatically determined relative to the GCL border and the INL border with an algorithm written in Matlab (Math Works). The GCL border (0% depth) was defined as the depth at which DAPI fluorescence peaked in the GCL (Figure 1D), and the INL border (100% depth) was defined as the depth at which the DAPI florescence was 66% of the maximum measured in the INL (Figure 1D). Dendritic depths were calculated locally near each dendritic segment to eliminate artifacts caused by the fact that the retina is not entirely flat. To reconstruct the detailed 3D morphology of PRV-labeled amacrines cells that were further away from the ganglion-cell body, we acquired several overlapping image stacks and stitched them together with an algorithm that calculated the correlation between neighboring frames in the ganglion-cell layer of DAPI-labeled stacks. The stitching algorithm was implemented in Mathematica (Wolfram Research). 3D visualization for Figure 1C and Figure 2C was done in Imaris (Bitplane). Colocalization of calretinin and GFP in the INL was quantified by the following algorithm in Mathematica: Confocal scans were acquired at a number of locations in the INL for DAPI, calretinin, and GFP. From the DAPI scan, the location of every cell nucleus was determined. Next, the GFP and calretinin channels were thresholded and for each nucleus the number of GFP- and/or calretinin-positive pixels around the nucleus were counted in a fixed window and plotted in Figure S3B. The horizontal axis shows the number of GFP-positive pixels and the vertical axis shows the number of calretinin-positive pixels for each cell.

Electrophysiology

Three to six days after PRV152 injection into the AntC of the right eye, the left eye was removed and the retina was dissected. The isolated retina was continuously superfused at a rate of 1 ml/min with Ames (pH 7.4) solution at 36°C and equilibrated with 95% O_2 and 5% CO_2. We recorded inhibitory currents from GFP-labeled ganglion cells under a voltage clamp with electrodes (5–8 MΩ) that were filled with 113 mM $CsMeSO_4$, 1 mM Mg SO_4, 7.8 mM 10^{-3} $CaCl_2$, 0.1 mM BABTA, 10 mM HEPES, 4 mM ATP-Na_2, 0.5 mM GTP-Na_3, 5 mM QX314-Br, and 7.5 mM Neurobiotin-Cl at pH 7.2 with a Multiclamp 700B patch-clamp amplifier (Axon Instruments). GFP-labeled ganglion cells were visualized by two-photon laser confocal imaging. Inhibitory currents were measured by clamping the membrane to 0mV, the reversal potential for ionotropic glutamate receptors. The recorded change of currents in the voltage clamp at 0 mV is proportional to the change of inhibitory conductance. (See more details in [S6, S7].) QX314 was used to block sodium currents internally. The visual-stimulation and data-acquisition software, Presentinator, was written in LabView (National Instruments) in the laboratory of F. Werblin at the University of California, Berkeley. Data were analyzed in Mathematica. Visual stimuli were applied with a digital light

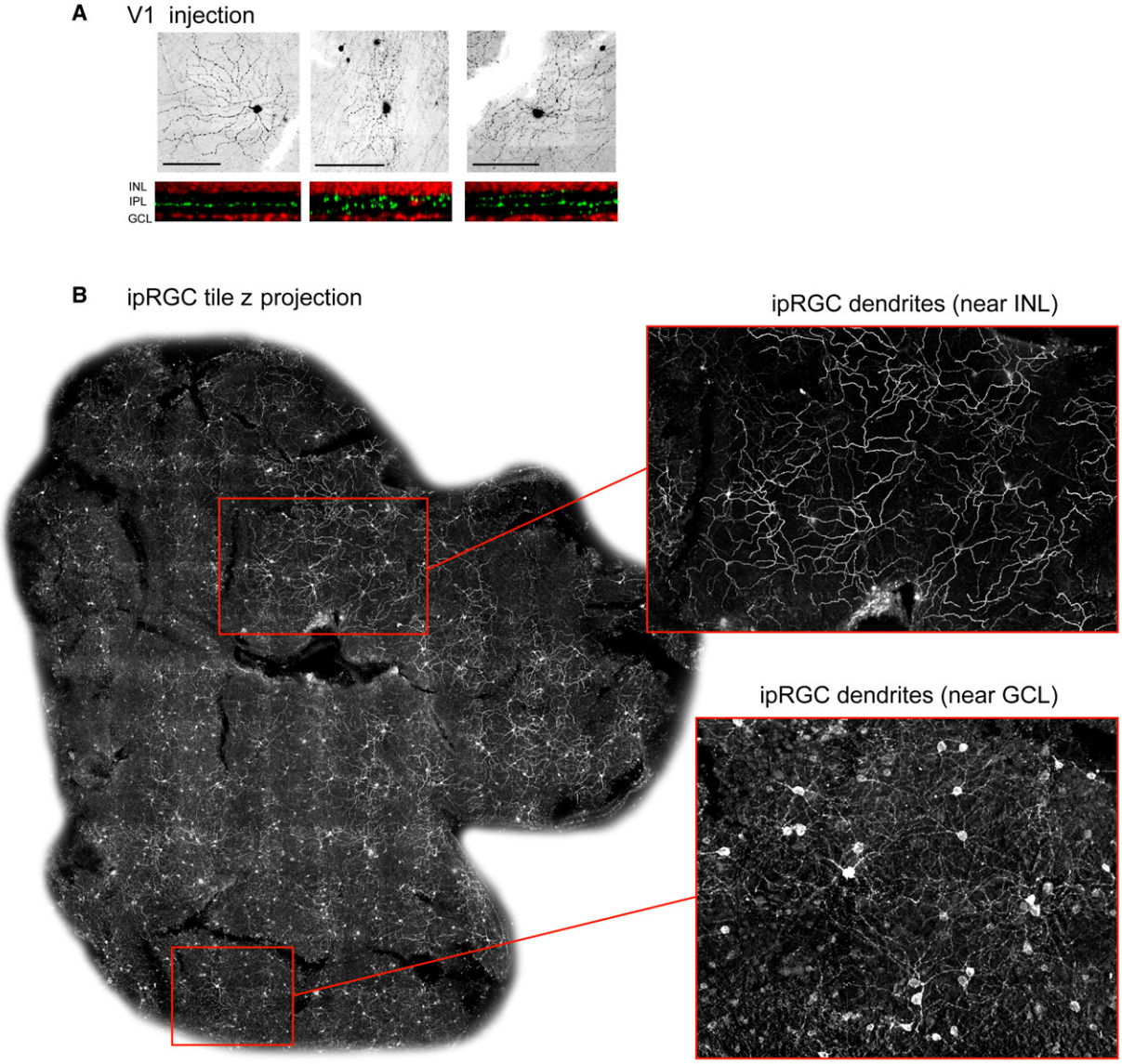

Figure S1. Morphological Subtypes of Retinal Ganglion Cells

(A) Examples of GFP-labeled ganglion cells 4 days after PRV152 injection into the SC. Side views are shown below top views and indicate dendritic stratification in the IPL between the INL and GCL (marked by DAPI, red). Scale bars represent 100 μm.

(B) Confocal z projection of a retina montage stained with melanopsin antibody (left). The scale bar represents 500 μm. Note that type 1 ipRGCs were the most intensely melanopsin-stained cells. Right: A magnification of two strata in the IPL closer to INL (above) and GCL (below) is shown. Both type 1 and type 2 cells covered and tiled the retina. Mean dendritic diameters were 410 ± 28 μm (type 1) and 230 ± 52 μm (type 2) with a mean distance between cell bodies of 250 ± 59 μm (type 1) and 95 ± 36 μm (type 2). The coverage factors for type 1 and type 2 cells were 2.5 and 4.8, respectively. Type 3 cells were not quantified.

processor (DLP) projector through the lamp port of a Nikon Eclipse 600 upright microscope. The image was focused on the photoreceptors through the condenser before the experiment.

Two-Photon Imaging

A two-photon laser-scanning confocal microscope was used to visualize GFP-labeled neurons in the retina in order to avoid bleaching of the photoreceptors. A 920 nm laser line from a 5W Millennia Pro pumped Tsunami laser (Spectra Physics) was attenuated by polarization optics and a Pockels cell (Conoptics, Model 302) and was scanned with mirrors (Cambridge Technologies) mounted on a modified Nikon Eclipse 600 upright microscope. The laser energy at the position of the retina was 5–20 mW. The acquisition software, Tango, was written by Florian Engert, Harvard University (Cambridge, MA).

For time-lapse imaging, the retina was superfused (as described above) for one day, and at every hour or half hour a Z stack of 80 images was acquired with 1 μm spacings. At the end of the time-lapse imaging, the retina was fixed in 4% paraformaldehyde in PBS and stained with antibodies for visualization of the circuit at a higher resolution.

Supplemental References

S1. Smith, B.N., Banfield, B.W., Smeraski, C.A., Wilcox, C.L., Dudek, F.E., Enquist, L.W., and Pickard, G.E. (2000). Pseudorabies virus expressing enhanced green fluorescent protein: A tool for in vitro electrophysiological analysis of transsynaptically labeled neurons in identified central nervous system circuits. Proc. Natl. Acad. Sci. USA *97*, 9264–9269.

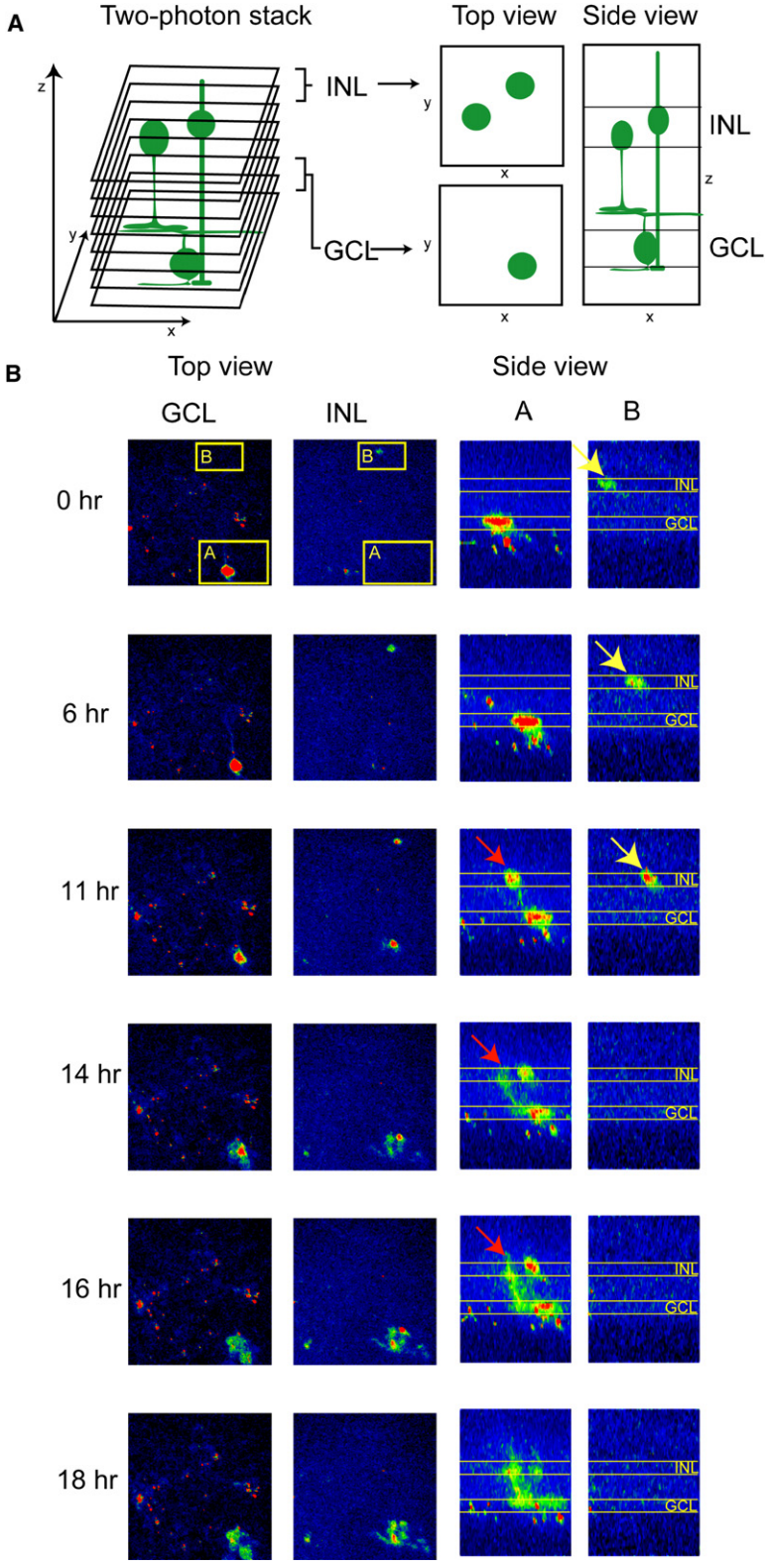

Figure S2. Time-Lapse Two-Photon Laser Imaging of the PRV152 Spread in the Retina, Showing that Infection of Amacrine and Müller Cells Is Temporally and Spatially Independent

Previously it was shown that PRV infection can spread from axons to glial cells that are in intimate contact with axons in the rat optic nerve but does not spread from these glial cells to other neurons [S8]. Therefore, glial cells have been proposed to be antiviral and unable to propagate PRV infection to other cells. Here we tested the temporal order of amacrine-Müller-cell PRV labeling to verify that amacrine cells are not labeled with PRV released from Müller cells. To rule this out, we argued that amacrine cells must either become GFP labeled earlier than Müller cells or become labeled at the same time but separated in space. We isolated retinas from the contralateral eye 3.5–4 days after PRV infection. At this stage of viral spread, only a few well-separated ganglion cells were labeled with GFP. The retina was maintained in an oxygenated superfusion chamber and two-photon confocal stacks were acquired (with 1 μm spacing) from regions around labeled ganglion cells every hour for 1–2 days with a two-photon laser microscope (see Experimental Procedures). The left panel in (A) shows a schematic picture of a GFP-labeled circuit and its corresponding acquired confocal stack. On the right, the images that were acquired for the GCL or INL are projected into the x-y plane and represent the GCL and INL, respectively (top views). The side view is the projection of the images on the x-z plane, where z represents the depth in the retina. Circuit 1 (B) shows the time-lapse imaging of GFP fluorescence. Each row shows a different time point (hr). The entire movie is shown in Movie S1. The first two columns show top views (x-y projections) of the GCL and INL (as in [A]). On the first row, areas A and B are highlighted. The last two columns show side views (x-z projections) of the highlighted areas A and B. The INL and GCL are highlighted by yellow lines. Area A shows a ganglion cell in the GCL and, later, Müller cells in the INL (red arrows). Area B shows an amacrine cell in the INL (yellow arrows). This amacrine cell is labeled before the Müller cells appear at 11 hr. The amacrine cell loses GFP fluorescence at 14 hr. The lateral shift in position is due to slow movement of the retina. We observed no temporal order between amacrine- and Müller-cell GFP expression; occasionally amacrine cells became GFP positive before Müller cells. In other cases, when amacrine cells became GFP positive after Müller cells, the two cell types were spatially separated. Infection of amacrine and Müller cells is therefore temporally and spatially independent (B). This observation suggests that amacrine cells are not infected with the PRV released from Müller cells.

S2. Banfield, B.W., Kaufman, J.D., Randall, J.A., and Pickard, G.E. (2003). Development of pseudorabies virus strains expressing red fluorescent proteins: New tools for multisynaptic labeling applications. J. Virol. *77*, 10106–10112.

S3. De Paola, V., Arber, S., and Caroni, P. (2003). AMPA receptors regulate dynamic equilibrium of presynaptic terminals in mature hippocampal networks. Nat. Neurosci. *6*, 491–500.

S4. Boldogkoi, Z., Reichart, A., Toth, I.E., Sik, A., Erdelyi, F., Medveczky, I., Llorens-Cortes, C., Palkovits, M., and Lenkei, Z. (2002). Construction of recombinant pseudorabies viruses

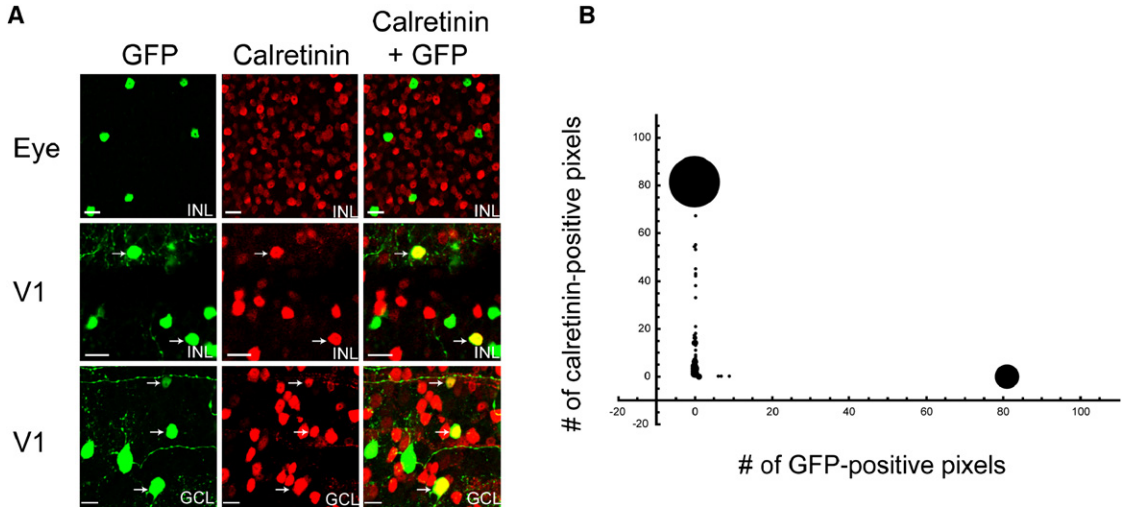

Figure S3. PRV Infection from ipRGCs Does Not Diffuse across Retinal Strata

To rule out the possibility that amacrine cells are infected by the nonsynaptic release of PRV152 from ganglion cells, we investigated GFP expression in amacrine-cell subtypes that occupied different strata than the PRV152-labeled ganglion-cell dendrites. We used the finding that the antibody against calretinin labels a subset of amacrine cells with processes in three distinct strata [S9]. These calretinin strata are different from the strata where GFP-positive ganglion dendrites ramify (see Figure 1D). Therefore, there are no calretinin-positive amacrines that make synapses in the strata where the GFP-labeled ganglion-cell dendrites ramify. If the virus spreads only transsynaptically from ganglion cells to amacrine cells, all GFP-positive amacrine cells should be calretinin negative. Conversely, if the virus is released from the ganglion-cell dendrites nonsynaptically, it could diffuse to neighboring strata and infect other cells in those strata. In this case, one should find calretinin-positive amacrine cells that are also GFP positive. To differentiate between the two possibilities, we double-labeled retinas, 5 days after infection from the contralateral eye (top row in [A]), with antibodies against GFP (green) and calretinin (red). None of the amacrine cells was double labeled, suggesting that PRV infection did not diffuse to neighboring strata from infected ganglion-cell dendrites. To rule out the possibility that PRV152 infection interfered with calretinin expression, we also double-stained retinas 4 days after V1 infection (middle and bottom rows in[A]). In this case, a number of ganglion and amacrine cells were double labeled. The focal plane is shown in the bottom right corner of each image. Arrows point to double-labeled cells. Scale bars represent 15 μm. We also quantified the calretinin and GFP colocalization in the INL after virus injection to the contralateral eye, on the basis of confocal scans, as in (A). For each cell, the horizontal axis shows GFP staining, and the vertical axis shows calretinin staining. Each point represents one cell or, if they have the same coordinates, multiple cells. The diameter of a point is proportional to the number of cells with the same coordinates. Cells with (0, 0) coordinates are not shown. No colocalization was detected. These findings support the contention that amacrine cells are infected only by transsynaptic spread from ganglion cells.

optimized for labeling and neurochemical characterization of neural circuitry. Brain Res. Mol. Brain Res. *109*, 105–118.

S5. Rabut, G., and Ellenberg, J. (2004). Automatic real-time three-dimensional cell tracking by fluorescence microscopy. J. Microsc. *216*, 131–137.

S6. Roska, B., and Werblin, F. (2001). Vertical interactions across ten parallel, stacked representations in the mammalian retina. Nature *410*, 583–587.

S7. Roska, B., and Werblin, F. (2003). Rapid global shifts in natural scenes block spiking in specific ganglion cell types. Nat. Neurosci. *6*, 600–608.

S8. Tomishima, M.J., and Enquist, L.W. (2002). In vivo egress of an alphaherpesvirus from axons. J. Virol. *76*, 8310–8317.

S9. Haverkamp, S., and Wässle, H. (2000). Immunocytochemical analysis of the mouse retina. J. Comp. Neurol. *424*, 1–23.